

Data Fusion Calibration for a 3D Laser Range Finder and a Camera using Inertial Data

P. Núñez, P. Drews Jr, R. Rocha and J. Dias

Abstract—The use of 3D laser range finder (LRF) and cameras is increasingly common in the navigation application for mobile robots. This paper proposes a new method to perform the extrinsic calibration between a pinhole camera and a 3D-LRF with the aid of an Inertial Measurement Unit (IMU). While state of the art calibration procedures require a large number of points for robust calibration, the proposed approach is innovative in terms of higher flexibility and wider range of application. The proposed method is based on the presentation to the sensor platform of a stationary planar board containing a checkerboard pattern. The homography which defines the rotation matrix between the LRF and camera is achieved moving the robot and observing the resulting motion of the sensors. This step attempts to solve the well-known homogeneous transform equation of the form $AX = BX$. Next, translation is calculated using a commonly least-squares estimation algorithm according to the corners of the pattern, previously detected by both, camera and LRF. The developed algorithm was tested on a mobile robot which is equipped with sensor platform composed of pinhole camera, LRF pan-tilt unit and a IMU, and proved to be very accurate. Furthermore, the applicability of the method is greatly expanded, requiring attachment of a simple inertial sensor to the sensor platform.

Index Terms - 3D Laser Sensors, Laser-Camera Calibration

I. INTRODUCTION

Simultaneous Localization and Mapping (SLAM) is an essential ability for autonomous mobile robots exploring unknown environments. In the last two decades, SLAM problem has been discussed in depth using two dimensional sensors (e.g. laser range finder, stereo camera or sonar). Currently, reliable mapping and self-localization in three dimensions, while the robot is moving in indoor or outdoor environments, are increasingly important tasks in the robotic field [1]. To achieve this 3D-SLAM, autonomous robots are usually equipped with sensors, e.g. 3D laser range finder (LRF), which acquires information of the robot environment. In this regard, some techniques for acquiring 3D data using 2D scanners installed on mobile robots have been developed [2], [3]. On the other hand, the efficiency and robustness of the SLAM process is determined by the chosen map representation and the data association stage [4]. In order to reduce this crucial problem, it is possible to augment the 3D data with other kind of information, such as color, which is able to be acquired by a single camera. To accomplish this, the laser range finder (LRF) and the cameras that

equip the robots must be extrinsically calibrated, that is, the rigid transformation between the camera and laser coordinate reference frames must be known.

Previous work regarding the laser-camera calibration issue focus on calibrating the cameras to 2D laser range finders with both visible and invisible trace [5]. A method to perform the calibration was presented by Zhang and Pless [6] which was based on the constraints between views of a planar calibration pattern like the ones used for the intrinsic camera calibration. This method's calibration error is affected by the angle between the LRF slice plane and the checkerboard plane, therefore the checkerboard needs to be placed at a specific orientation. Another approach from Li *et. al.* [7] is based on the line constraint equation obtained using a specially designed triangular checkerboard calibration pattern.

The recent development of 3D laser range finders made the use of these scanners more common, even though it still brings some disadvantages, namely some lack of flexibility and the time cost of data acquisition. Nevertheless, 3D scanners are well suited for particular tasks. Some previous work has been done regarding the 3D laser-camera calibration namely by Unnikrishnan and Herbert [8]. Their method uses a checkerboard as calibration pattern and several laser-camera acquisitions. Another method to perform the extrinsic calibration, developed by Scaramuzza *et. al.* [9], obviates the need to have a calibration pattern and uses only point correspondences, hand selected by the user, from a single laser-camera acquisition.

This paper also presents a method for the extrinsic calibration between a 3D LRF and a camera, but an inertial measurement unit (IMU) has been added to the sensor platform (see Fig. 1). Previous approaches need a large number of points for a robust calibration. However the proposed method allows to obtain the calibration in a faster and easier way, only using this IMU sensor. A stationary planar board containing a checkerboard pattern is presented to the sensor platform. The method is based on the classical hand-eye calibration [10]. In the proposed approach, the inertial sensor provides information regarding the orientation of the sensor platform, thus restricting the calibration problem. Therefore, the homography between the LRF and the camera is determined by moving the robot and analyzing the IMU and camera information. This yields a homogeneous transform equation of the form $AX = XB$, where A is the change between the robot pose (using the IMU) and B the resulting camera displacement.

The required translation vector is obtained by associating a restrict set of points that are obtained on both the LRF scan

P. Núñez is member of the ISIS Group, Dpto. Tecnología Electrónica, Universidad de Málaga, and is with Dept. Tecnología de los Computadores y las Comunicaciones, Univ. de Extremadura, Spain (e-mail: pmnt@uma.es).

The other authors are with the Institute of Systems and Robotics, Dept. Electrical and Computer Engineering, Univ. of Coimbra, Portugal.

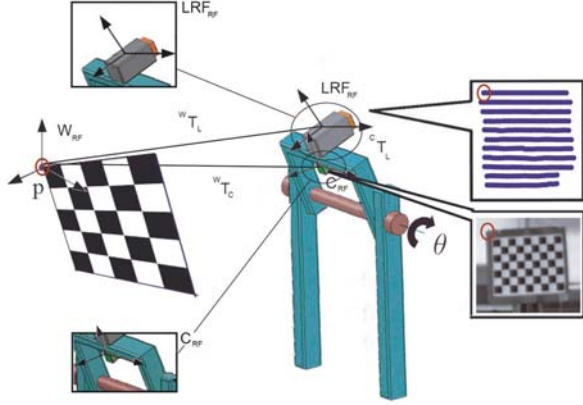


Fig. 1. A schematic of the calibration problem. The main goal of the paper is to achieve a calibration method to obtain the rigid transformation between the information acquired by a LRF and the pinhole camera.

and camera capture. These points are the outer vertexes of the calibration pattern. Taking into account that the rotation is acquired in a fast and accurate way, the translation is estimated only using an iterative method based on these outer points, which is easy to implement.

This document has been organized as follows. Section II describes the geometric models of the camera, 3D laser and inertial measurement unit. Next, Section III describes four techniques for the calibration of the 3D-LRF and camera. Finally, experimental results, and conclusions and future work are described in Section IV and Section V, respectively.

II. SENSOR PLATFORM PROJECTION MODEL

The goal of the method is to find the homogeneous transformation between the pinhole camera and the LRF (${}^C\mathbf{T}_L$) in order to fuse the measurements from both sensors in robotic applications. The sensor platform consists of a 3D-LRF, a pinhole camera and an inertial measurement unit. The schematic of the proposed method is shown in Fig. 1. As it is shown in the figure, the 3D scan data acquisition is achieved using a 2D-LRF and a tilt-unit. Three coordinate frames, namely camera (C_{RF}), laser range finder (LRF_{RF}) and the world (W_{RF}) have been defined in Fig. 1. A checkerboard pattern is presented to the robot and the outer points are extracted by both camera and 3D-LRF. Next, the geometric models of the different sensors of the platform are described.

A. Camera Geometric Model

In the proposed approach, a pinhole camera has been used. These cameras are modeled by their optical center and their image plane. Assuming that the camera is already calibrated, a given 3D point \mathbf{W} is projected into an image point \mathbf{M} given by the intersection of the line containing the optical center and \mathbf{W} with the image plane [11].

Let $\mathbf{w} = (x, y, z)^T$ be the coordinates of \mathbf{W} in the world reference frame and \mathbf{m} the coordinates of \mathbf{M} in the image plane. Using projective coordinates,

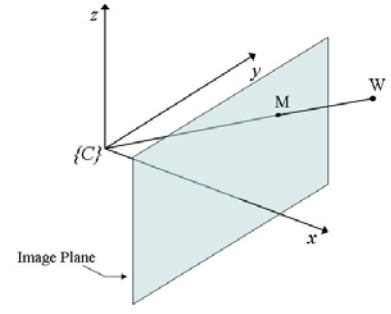


Fig. 2. Pinhole camera model. The point in the world W is projected into the image plane M according to the intrinsic parameters of the camera.

$$\tilde{\mathbf{w}} = \begin{bmatrix} x \\ y \\ z \\ 1 \end{bmatrix} \quad \tilde{\mathbf{m}} = \begin{bmatrix} u \\ v \\ 1 \end{bmatrix} \quad (1)$$

the transformation from $\tilde{\mathbf{w}}$ to $\tilde{\mathbf{m}}$ is given by the matrix $\tilde{\mathbf{P}}$:

$$\lambda \tilde{\mathbf{m}} = \tilde{\mathbf{P}} \tilde{\mathbf{w}} \quad (2)$$

where λ is the depth (arbitrary scale) factor. The camera is therefore modeled by its *perspective projection matrix* (PPM) $\tilde{\mathbf{P}}$, which can be decomposed using the QR factorization

$$\tilde{\mathbf{P}} = \mathbf{A} [\mathbf{R} \mid \mathbf{t}] \quad (3)$$

The matrix \mathbf{A} depends on the *camera intrinsic parameters* and has the following form:

$$\mathbf{A} = \begin{bmatrix} \alpha_u & \gamma & u_0 \\ 0 & \alpha_v & v_0 \\ 0 & 0 & 1 \end{bmatrix} \quad (4)$$

where $\alpha_u = -fk_u$ and $\alpha_v = -fk_v$ are the focal lengths in horizontal and vertical pixels (f is the focal length in millimeters, k_u and k_v are the effective number of pixels per millimeter along the u and v axes). (u_0, v_0) are the coordinates of the *principal point*, given by the intersection of the optical axis (z) with the image plane, γ is the *skew factor*.

The camera *extrinsic parameters* are encoded by the 3×3 rotation reference frame onto the world reference frame.

Using quaternions and writing the PPM as:

$$\tilde{\mathbf{P}} = \begin{bmatrix} \mathbf{q}_1^T & q_{14} \\ \mathbf{q}_2^T & q_{24} \\ \mathbf{q}_3^T & q_{34} \end{bmatrix} \quad (5)$$

the projection (2) in Cartesian coordinates is given by:

$$\begin{cases} u = \frac{\mathbf{q}_1^T \mathbf{w} + q_{14}}{\mathbf{q}_3^T \mathbf{w} + q_{34}} \\ v = \frac{\mathbf{q}_2^T \mathbf{w} + q_{24}}{\mathbf{q}_3^T \mathbf{w} + q_{34}} \end{cases} \quad (6)$$

The *focal plane* is parallel to the image plane and contains the optical center (\mathbf{C}) (Fig. 2). The focal plane is also the focus of the points projected to infinity, therefore its equation

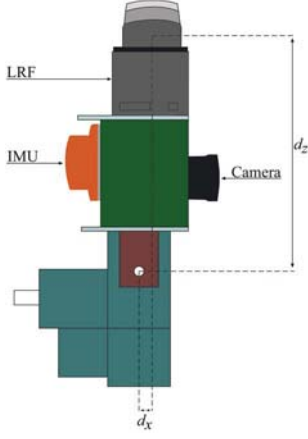


Fig. 3. Sketch of the measurement system (d_x and d_z are the offset distances from the rotation axis to the center of the laser mirror)

is $\mathbf{q}_3^T + q_{34} = 0$. The two planes defined by $\mathbf{q}_1^T \mathbf{w} + q_{14} = 0$ and $\mathbf{q}_2^T \mathbf{w} + q_{24} = 0$ intersect the image plane respectively in the vertical and horizontal axis of the image coordinates.

The optical center \mathbf{C} is the intersection of these three planes, therefore its coordinates \mathbf{c} are the solution of

$$\tilde{\mathbf{P}} \begin{bmatrix} \mathbf{c} \\ 1 \end{bmatrix} = 0 \quad (7)$$

then

$$\mathbf{c} = -\mathbf{Q}^{-1} \tilde{\mathbf{q}} \quad (8)$$

being \mathbf{Q} and $\tilde{\mathbf{q}}$ defined in (5) as the first and second columns, respectively. Thus, from (8) $\tilde{\mathbf{P}}$ is written

$$\tilde{\mathbf{P}} = [\mathbf{Q} \mid -\mathbf{Q}\mathbf{c}] \quad (9)$$

The *optical ray* associated to an image point \mathbf{M} is the line \mathbf{MC} . The equation of this ray can be written as:

$$\mathbf{w} = \mathbf{c} + \lambda \mathbf{Q}^{-1} \tilde{\mathbf{m}} \quad (10)$$

B. LRF Geometric Model

A 3D laser range finder is usually built by moving a 2D LRF along one of its axes. By rotating the 2D scanner around its radial axis it is possible to obtain the spherical coordinates of the points measured. This construction of the laser creates a problem, it is not possible to adjust the center of rotation of the laser mirror with the center of rotation of the laser itself (see Fig. 3). Therefore, offsets on the measured points will exist [9]. The 3D LRF used in the proposed work was built using a 2D Hokuyo laser mounted on a Directed Perception pan-tilt unit. This type of configuration for the 3D laser can be modeled by Eq. (11).

$$\begin{bmatrix} x \\ y \\ z \end{bmatrix} = \begin{bmatrix} c_i c_j & -c_i s_j & s_i & c_i d_x + s_i d_z \\ s_j & c_j & 0 & 0 \\ -s_i c_j & s_i s_j & c_i & -s_i d_x + c_i d_z \end{bmatrix} \begin{bmatrix} \rho_{ij} \\ 0 \\ 0 \\ 1 \end{bmatrix}$$

$$c_i = \cos(\varphi_i), c_j = \cos(\theta_j), s_i = \sin(\varphi_i), s_j = \sin(\theta_j), \quad (11)$$

where ρ_{ij} is the j -th measured distance with corresponding orientation θ_j in the i -th scan plane, which makes the angle φ_j with the horizontal plane. The offset of the rotation axis from the center of the mirror has components d_x and d_z . $[x \ y \ z]^T$ are the coordinates of each point measured relative to the center of rotation of the laser, with the x axis pointing forward and the z axis pointing up.

C. Inertial Sensor Data

At a basic level, an inertial system performs a double integration of sensed acceleration over time to estimate the position [12]. Assuming that acceleration is measured along three orthogonal axis, then

$$x = \int \dot{x} dt = \int \int \ddot{x} dt = \int \int a_{sensed} dt \quad (12)$$

where x is the position, \dot{x} is the velocity and \ddot{x} is the acceleration vectors.

If the quaternion $\hat{\mathbf{q}}(k)$ represents the body rotation relative to the navigation frame at sample interval k , then the body accelerations can be converted to the navigation frame of reference by

$$\mathbf{a}_{nav} = \hat{\mathbf{q}}(k) \mathbf{a}_{body} \hat{\mathbf{q}}(k)^* \quad (13)$$

The set of orthogonal gyros provide a measurement of the body rotation rate vector given by

$$\boldsymbol{\omega} = [\omega_x \ \omega_y \ \omega_z]^T \quad (14)$$

and $\|\boldsymbol{\omega}\| = \sqrt{\omega_x^2 + \omega_y^2 + \omega_z^2}$ gives the magnitude of the rotation rate and $\frac{\boldsymbol{\omega}}{\|\boldsymbol{\omega}\|}$ the unit vector around which the rotation occurs. The rotation increment during a sampling interval Δt is given by the quaternion

$$\Delta \hat{\mathbf{q}} = \cos\left(\frac{\boldsymbol{\omega} \Delta t}{2}\right) - \sin\left(\frac{\boldsymbol{\omega} \Delta t}{2}\right) \frac{\boldsymbol{\omega}}{\|\boldsymbol{\omega}\|}, \quad (15)$$

provided that $\|\boldsymbol{\omega}\| \neq 0$. The quaternion $\hat{\mathbf{q}}(k)$, that represents the body rotation relative to the navigation frame at sample interval k , can now be updated by

$$\hat{\mathbf{q}}(k+1) = \hat{\mathbf{q}}(k) \Delta \hat{\mathbf{q}}, \quad (16)$$

and, using (13), the measured body accelerations are converted to the navigation frame, the gravity component is removed, and integration provides body velocity and position in the navigation frame.

The inertial sensor calculates the orientation between the sensor-fixed coordinate system, $\{S\}$, and the earth-fixed reference coordinate system, $\{G\}$. By default $\{G\}$ is defined as a right handed Cartesian coordinate system with: X positive when pointing to the local magnetic North, Y according to the right handed coordinates (West) and Z positive when pointing up (see figure 4).

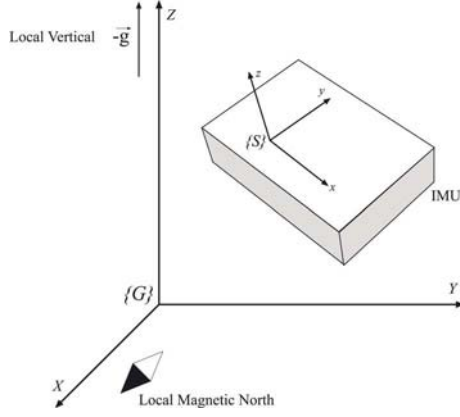


Fig. 4. IMU coordinates. Inertial sensor has been used to provide information regarding the orientation of the sensor platform

D. Relation between LRF-Camera using IMU

On this section we will use a derivation of the formulation described by Ferreira [13] used to build a scanner to perform 3D registration of objects, where a pose system was used to provide rotation and translation information between coordinate reference systems. On the proposed approach, an inertial sensor will be used instead of a pose one. This means translation information between coordinate systems cannot be readily obtained.

The coordinate reference systems used on the calibration are defined as follows: $\{W_{RF}\}$ is the world coordinate system associated with the calibration checkerboard pattern, $\{LRF_{RF}\}$ and $\{C_{RF}\}$ are the laser and camera coordinate systems respectively and $\{G\}$ is the earth-fixed coordinate system. Since the IMU is rigidly coupled to the sensors platform and only orientation information is used, it is possible to assume the inertial sensor rotation information to be relative to the laser coordinate system.

Let P_W be the coordinates of a point in the world coordinate system and P_L and P_C the coordinates of the same point in the laser and camera coordinate systems, respectively. Then

$$P_W = {}^W\mathbf{T}_L \cdot P_L = {}^W\mathbf{T}_C \cdot P_C, \quad (17)$$

where ${}^W\mathbf{T}_L$ is the rigid transformation from the laser coordinate system to the world coordinate system and ${}^W\mathbf{T}_C$ is the rigid transformation from the camera coordinate system to the world coordinate system.

Figure 5 shows the relation between the coordinate systems transformations that can be written as

$${}^W\mathbf{T}_L = {}^W\mathbf{T}_C \cdot {}^L\mathbf{T}_C^{-1} \quad (18)$$

applying the previous relation to (17) we obtain

$$P_L = {}^L\mathbf{T}_C \cdot P_C \quad (19)$$

Since the inertial sensor will only provide information about the relative rotations we will write the transformations as

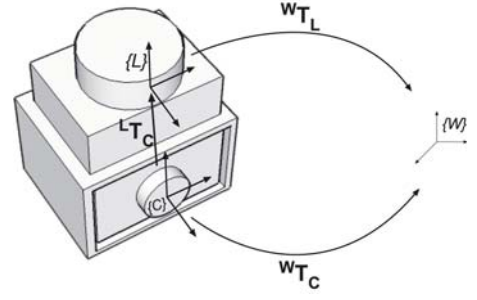


Fig. 5. Transformations between different coordinate systems

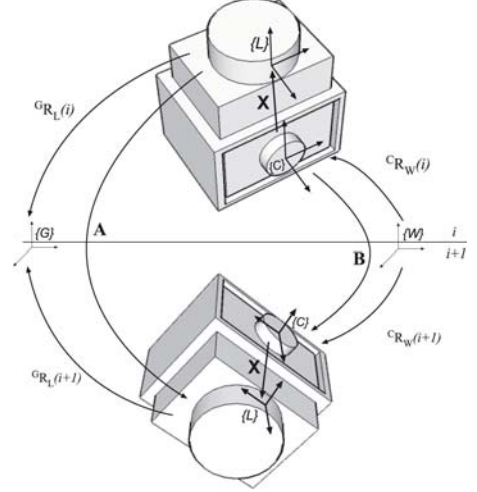


Fig. 6. Relative motion schematic during calibration procedure on two different time instant.

$$\begin{aligned} {}^W\mathbf{T}_L &= \begin{bmatrix} {}^W\mathbf{R}_L & {}^W\vec{\mathbf{t}}_L \end{bmatrix} \\ {}^W\mathbf{T}_C &= \begin{bmatrix} {}^W\mathbf{R}_C & {}^W\vec{\mathbf{t}}_C \end{bmatrix} \end{aligned} \quad (20)$$

where \mathbf{R} are the rotations and $\vec{\mathbf{t}}$ are the translations between coordinate systems.

Figure 6 shows a schematic for the relative motion of the sensors during calibration on two different time instants. Because the laser and the camera are rigidly coupled it is possible to write the following equation

$$\mathbf{A}\mathbf{X} = \mathbf{X}\mathbf{B}, \quad (21)$$

where \mathbf{A} and \mathbf{B} are the relative rotation transformations from the time instant i to the time instant $i+1$, and \mathbf{X} is the rotational transformation between the laser and the camera (see Fig. 6). Since we have rotation information from the inertial sensor we will express \mathbf{A} , \mathbf{B} and \mathbf{X} through Eq. (22).

$$\begin{aligned} \mathbf{A} &= {}^G\mathbf{R}_L^{-1}(i+1) {}^G\mathbf{R}_L(i) \\ \mathbf{B} &= {}^C\mathbf{R}_W(i+1) {}^C\mathbf{R}_W^{-1}(i) \\ \mathbf{X} &= {}^L\mathbf{R}_C \end{aligned} \quad (22)$$

\mathbf{A} is obtained directly using the inertial sensor information of two consecutive captures and \mathbf{B} is also easily obtained

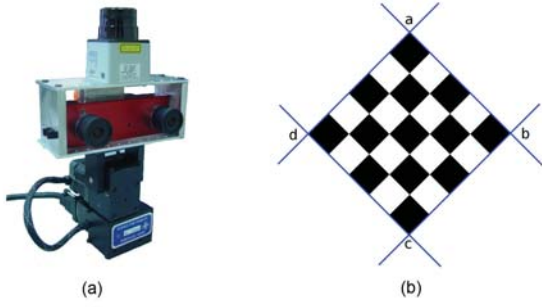


Fig. 7. a) Pan and tilt unit with a stereo-camera rig, an IMU and an Hokuyo LRF mounted on top. Left camera of the pair stereo is the pinhole camera used in the proposed approach; and b) calibration pattern which is presented to the robot.

from the captures once the Camera is calibrated. Shiu and Ahmad [14] presented a closed-form solution to the homogeneous transformation equation (21) although a more compact solution can be achieved using quaternion algebra as discussed in [15], [10]. Therefore we will write (21) as

$$\hat{\mathbf{a}} * \hat{\mathbf{q}} = \hat{\mathbf{q}} * \hat{\mathbf{b}}, \quad (23)$$

where $\hat{\mathbf{a}}$, $\hat{\mathbf{b}}$ and $\hat{\mathbf{q}}$ are the quaternions that correspond to the rotations given by \mathbf{A} , \mathbf{B} and \mathbf{X} respectively. Once ${}^L R_C$ is calculated, the translation vector is estimated by associating the outer vertexes of the calibration pattern using a commonly least-squares estimation algorithm.

III. ITERATIVE CALIBRATION AND OPTIMIZATION

Figure 7b shows how the calibration pattern should be presented to the sensor platform. In the figure, outer vertexes have been illustrated. As it was drawn in Fig. 6, two robot motion are needed, and then, two full 3D scan data are collected. In order to reduce the errors in the estimate of the homogeneous transformation ${}^L R_C$, the procedure is repeated N times for different α angles, in which the checkerboard is visible (steps from 2) to 5)) [10]. The calibration algorithm developed is summarized as follows:

- 1) Calibrate the Camera using [16].
- 2) For two sensors positions retrieve the rotations given by the inertial sensor and the rigid transformations from the camera reference frame to the checkerboard reference frame.
- 3) Determine ${}^L R_C$ using (23) and applying the method described briefly in Section II-D (see more details in Horaud's work [10]).
- 4) From the laser scan find the points \mathbf{a} , \mathbf{b} , \mathbf{c} and \mathbf{d} by detecting the intersection of the lines \overline{ab} , \overline{bc} , \overline{cd} and \overline{da}
- 5) With the information from 3) and 4) use (19) to determine ${}^L T_C$
- 6) Optimize the obtained result. Using the previous algorithm, a translation matrix for each corner of each pose of the calibration pattern is obtained. Thus, different results for the translation are estimated. This last step joins the information from 5) step of the N iterations.

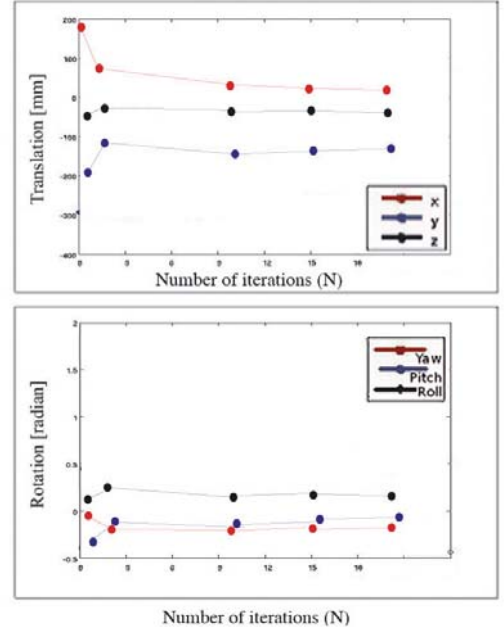


Fig. 8. Evolution of the rotation and translation matrices estimate by the calibration method according to the number of iterations used in the approach.

At the end of the calibration algorithm, the homogeneous transformation between the pinhole camera and the LRF (${}^C T_L$) is estimated.

IV. EXPERIMENTS AND RESULTS

The proposed approach was tested using the sensor platform shown in Fig. 7. The pinhole camera is selected from the left camera of STH-MDCS stereo pair from Videre Design, a compact, low-power colour digital stereo head with an IEEE 1394 digital interface. It consists of two 1.3 megapixel, progressive scan CMOS images mounted in a rigid body, and a 1394 peripheral interface module, joined in an integral unit (only one camera has been used for data acquisition). Images obtained were restricted to 320x240 pixels. The laser range finder mounted on the tilt unit is an Hokuyo URG-04LX, a compact laser sensor which has a resolution of 0.36° and the field of view of 240° . Furthermore, an MTi-G inertial sensor is strongly coupled to the laser range finder.

The average reprojection error values, in pixels, according to the number of iterations used in the method has been represented in Table I (Average and standard deviation values). As it is shown in Table I, the average error of the proposed calibration method decreases when the method use a higher number of iterations. The experiment has been repeated for different settings, deriving similar results. It is possible to consider that for $N = 10$ iterations, the calibration method is stable. These same results can be obtained analyzing the Fig. 8. In Fig. 8a-b, the evolution of the rotation and translation matrices have been shown, ${}^L R_C$ and ${}^L t_C$, respectively.

The accuracy of the method is shown in Fig. 9. Fig. 9a illustrates the 3D scan data acquired by the LRF in the calibration stage (9b). The checkerboard pattern has been

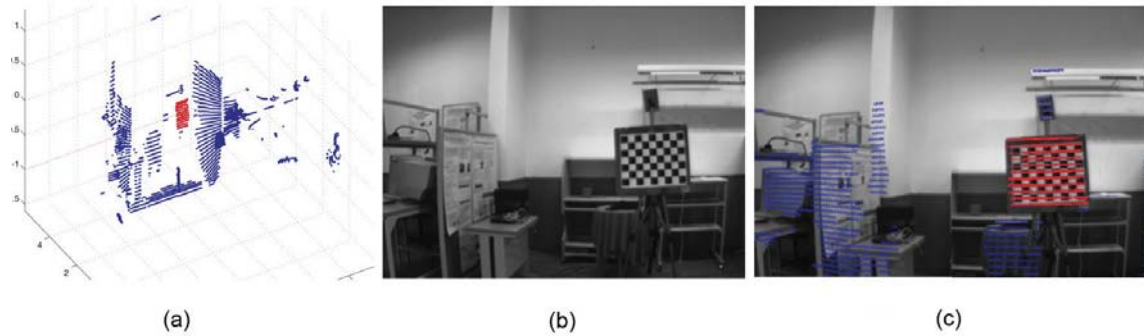


Fig. 9. a) 3D scan data acquired by the HOKUYO laser range finder in a real scenario which is used in the calibration procedure; b) image captured by the pinhole camera in the same scenario; and c) projection of the scan data over the image after the calibration process.

TABLE I

COMPARATIVE STUDY ACCORDING THE NUMBER OF VIRTUAL 3D POINTS. AE = AVERAGE ERROR SD = STANDARD DEVIATION (PIXELS)

	$N = 1$	$N = 3$	$N = 10$	$N = 15$	$N = 20$
AE	46.323	12.615	4.854	4.480	4.211
SD	8.312	4.277	3.121	3.108	2.935

drawn with red colour (rest of the scan data in blue colour). The projection of the 3D laser range data has been drawn over the image camera after the calibration process (9c). This experiment has been achieved in different scenarios with similar results. In this example, the proposed algorithm demonstrates its applicability for being used in 3D robotic applications.

V. CONCLUSIONS AND FUTURE WORKS

This paper has described an efficient method to calibrate a pinhole camera and a 3D laser range finder with the aid of an inertial sensor. The homography which defines the transformation between the sensors is achieved using a two steps method. First, the rotation matrix is estimated moving the robot and observing the resulting motion of the sensors. Next, translation is calculated using a commonly least-squares estimation algorithm according to the corners of the pattern, which have been previously detected by the camera and LRF, respectively. Therefore, the two sets of points are corresponded in order to obtain the homogeneous transformation between the camera pair and the range sensor. Experimental results have demonstrated the robustness, efficiency and applicability of the proposed solution. In fact, the approach described in this work requires no special equipment and allows to the researcher to calibrate quickly and in an accurate way the sensor platform. Future work will be focused on the application of this calibration method to projects related with 3D robotic applications (e.g. 3D-SLAM or virtual reconstruction of the robot environment).

VI. ACKNOWLEDGEMENTS

This work has been partially supported by the IRPS, EU-FP6-IST-045048 project, by the Spanish Ministerio de Ciencia e Innovación (MCINN) Project n. TIN2008-06196, HP2007-0005 and FEDER funds.

REFERENCES

- [1] D. Cole and P. Newman. "Using laser range data for 3D SLAM in Outdoor environment" *Proceedings of the IEEE International Conference on Robotics and Automation*, pp. 1556-1563, 2006.
- [2] D. Hahnel, W. Burgard and S. Thrun. Learning compact 3D models of indoor and outdoor environments with a mobile robot. *Robotics and Autonomous Systems*, 44(1):15-27, 2003.
- [3] O. Wulf, K. O. Arras, H., I. Christensen and Bernardo Wagner. "2D Mapping of Cluttered Indoor Environments by Means of 3D Perception". in *Proceedings of the International Conference on Robotics & Automation*, pages 4204-4209, 2004.
- [4] S. Roulmeliotis and G. A. Bekey. SEGMENTS: A layered, dual kalman filter algorithm for indoor feature extraction, in *Proc. IEEE/RSJ Int. Conf. on Intelligent Robots and Systems*, pp. 454-461, 2000.
- [5] C. Mei and P. Rives. "Calibration between a central catadioptric camera and a laser range finder for robotic applications", in *Proceedings of the IEEE International Conference on Robotics and Automation*, pages 532-537, 2006.
- [6] Q. Zhang and R. Pless. "Extrinsic calibration of a camera and laser range finder (improves camera calibration)", in *Proceedings of IEEE/RSJ International Conference on Intelligent Robots and Systems*, pages 2301-2306, 2004.
- [7] G. Li, Y. Liu, L. Dong, X. Cai, and D. Zhou. "An algorithm for extrinsic parameters calibration of a camera and a laser range finder using line features", in *Proceedings of the IEEE/RSJ International Conference on Intelligent Robots and Systems*, pages 3854-3859, 2007.
- [8] R. Unnikrishnan and M. Hebert. "Fast extrinsic calibration of a laser rangefinder to a camera", *Technical report, CMU-RI-TR-05-09*, Robotics Institute, Carnegie Mellon University, 2005.
- [9] D. Scaramuzza, A. Harati, and R. Siegwart. "Extrinsic Self Calibration of a Camera and a 3D Laser Range Finder from Natural Scenes", in *Proceedings of the IEEE International Conference on Intelligent Robots and Systems*, 2007.
- [10] R. Horaud and F. Dornaika. "Hand-eye calibration", *Int. Journal of robotic research*, Vol. 14(3), pp. 195-210, 1995.
- [11] A. Fusiello, E. Trucco, and A. Verri. "Rectification with unconstrained stereo geometry". In *Proceedings of the British Machine Vision Conference*, pp. 400-409, 1997.
- [12] Jorge Lobo. "Integration of Vision and Inertial Sensing". PhD thesis, Electrical and Computer Engineering Department, University of Coimbra, 2006.
- [13] Joao Filipe Ferreira. "Tele3d - um scanner para registo tridimensional de objectos". Master's thesis, Electrical and Computer Engineering Department, University of Coimbra, 2004.
- [14] Y. C. Shiu and S. Ahmad. "Calibration of wrist-mounted robotic sensors by solving homogeneous transform equations of the form $ax = xb$ ". *IEEE Transactions on Robotics and Automation*, pp 16U29, 1989.
- [15] H. Zhuang and Z. S. Roth. Comments on "calibration of wristmounted robotic sensors by solving homogenous transform equations of the form $ax = xb$ ". *IEEE Transactions on Robotics and Automation*, pp. 877U878, 1991.
- [16] Jean-Yves Bouguet. Camera Calibration Toolbox for Matlab: http://www.vision.caltech.edu/bouquetj/calib_doc/.